Broken pairs and evolution of collectivity in the A≅140 mass region: High spin states of the ^138_60Nd_78 nucleus

de Angelis, G.; Cardona, M. A.; De Poli, M.; Lunardi, S.; Bazzacco, D.; Brandolini, F.; Vretenar, Dario; Bonsignori, G.; Savoia, M.; Wyss, R.; ...

Source / Izvornik: **Physical Review C - Nuclear Physics, 1994, 49, 2990 - 2999**

Journal article, Published version
Rad u časopisu, Objavljena verzija rada (izdavačev PDF)

https://doi.org/10.1103/PhysRevC.49.2990

Permanent link / Trajna poveznica: https://urn.nsk.hr/urn:nbn:hr:217:598134

Broken pairs and evolution of collectivity in the $A \approx 140$ mass region: High spin states of the $^{138}_{60}Nd_{78}$ nucleus

G. de Angelis, M. A. Cardona, and M. De Poli
Istituto Nazionale di Fisica Nucleare, Laboratori Nazionali di Legnaro, Legnaro, Italy

S. Lunardi, D. Bazzacco, and F. Brandolini
Dipartimento di Fisica dell'Università, and Istituto Nazionale di Fisica Nucleare, Sezione di Padova, Padova, Italy

D. Vretenar
Physics Department, Faculty of Science, University of Zagreb, Zagreb, Croatia

G. Bonsignori and M. Savoia
Dipartimento di Fisica dell'Università and Istituto Nazionale di Fisica Nucleare, Sezione di Bologna, Bologna, Italy

R. Wyss
Royal Institute of Technology, Physics Department Frescati, Stockholm, Sweden

F. Terrasi and V. Roca
Dipartimento di Scienze Fisiche dell'Università, and Istituto Nazionale di Fisica Nucleare, Sezione di Napoli, Napoli, Italy
(Received 27 December 1993)

An in-beam γ-ray study performed with the ^{121}Sb (^{19}F,4n) reaction has established the high spin level structure of the $N = 78$ nucleus ^{138}Nd. States up to $I = 21\hbar$ and 8.5 MeV excitation energy have been identified. High spin states are described in the framework of the cranking model and of the interacting boson model with broken pairs. The calculations reproduce levels up to $I = 18\hbar$ including the two 10^+ states which, from the feeding cascades, are identified as the $\nu h^{-2}_{11/2}$ and $\pi h^2_{11/2}$ excitations. Cranked Strutinsky type calculations predict opposite shapes for the two different types of excitations.

PACS number(s): 23.20.Lv, 27.60.+j

I. INTRODUCTION

In all the even-even nuclei with mass number $A \approx 140$ the alignment of both neutron and proton quasiparticles in the $h_{11/2}$ orbital generates low-lying 10^+ states, in many cases isomeric. These excitations have been localized in the $N = 78$ ^{140}Sm and ^{142}Gd nuclei [1] and identified as the proton or neutron $h^2_{11/2}$ configurations through g-factor measurments [2]. Such states couple to the respective core excitations giving rise to $\Delta I = 2$ decoupled bands whose characteristic patterns allow one to identify the involved core and consequently to recognize, in an alternative way, the neutron or proton nature of the aligned $h^2_{11/2}$ configuration.

Rare-earth nuclei of this mass region are expected to be soft with resepct to the γ degree of freedom [3,4]. Shape transitions may therefore take place, due to the alignment of different quasiparticle states. In fact a single particle in a high-j shell generates a torus-shaped density distribution which induces an oblate shape of the nucleus, with the spin along the symmetry axis, driving the nucleus to $\gamma \geq 0°$. A single hole into a similar orbit tends to make the nucleus prolate with the spin along the symmetry axis, polarizing towards $\gamma \leq -60°$.

For $N = 78$ nuclei in the rare-earth region the high-j $h_{11/2}$ unique parity orbital is accessible to both neutron and proton excitations. Because of the different nature of these states (particle for the proton configuration and hole for the neutron configuration) opposite deformations are induced by such alignments due to the polarization of the soft core. This gives rise to the shape coexistence effects observed in many $N = 78$ isotones from Ce to Gd [1,5].

In this paper we report on an in-beam study of the $N = 78$ nucleus ^{138}Nd. The discussion of the experimental level scheme will proceed in three steps. In the first one the level sequences identified above the proton and neutron 10^+ excitations are compared with the level energies of neighboring nuclei. The evidence of the above-discussed shape transition will be compared with the prediction of cranked Strutinsky type calculations. Finally, for a quantitative comparison, in order to describe the high spin states the interacting boson model extended by the inclusion of noncollective fermion states (broken pairs) will be used. These calculations reproduce the $h^2_{11/2}$ proton and neutron alignments and the relative coupling to the core excitations.

II. MEASUREMENTS AND RESULTS

Low-lying states in ^{138}Nd have previously been discussed by Müller-Veggian *et al.* [6] who have identified a 0.41 μs 10^+ isomer with a suggested a $\nu h_{11/2}^{-2}$ configuration. We have now extended to higher spin the level scheme of ^{138}Nd using the ^{121}Sb(^{19}F,4n) reaction. The target consisted of 1 mg/cm^2 of isotopically enriched ^{121}Sb rolled on a natural Au backing of 5 mg/cm^2 to stop the recoiling nuclei. The ^{19}F beam was provided by the XTU Legnaro tandem with typical intensity of 5 particles nA on target. On the basis of the results of a short excitation function measurement, a beam energy of 75 MeV has been chosen for the subsequent γ-γ coincidence measurement. An array of six n-type Ge detectors with BGO anti-Compton shields was used to collect γ-γ coincidence data. Multiplicity and total γ-ray energy information was obtained using fourteen hexagonally shaped BaF_2 crystals in two groups of seven, vertically positioned above and below the target chamber, covering a solid angle of $\approx 70\%$. About 4×10^7 events were stored onto magnetic tape. The tapes were sorted off line in order to produce, after equalization of the germanium energy parameters, a symmetrized E_γ-E_γ matrix. The information from the BaF_2 detectors was used to suppress low multiplicity events from β decay and Coulomb excitation. Examples of background subtracted gated spectra generated from the E_γ vs E_γ matrix are shown in Fig. 1. Information on γ-ray multipolarities has been derived from angular correlation results selecting coincidence events between the two detectors positioned at angles close to 90° and the four positioned as close as possible to the beam line ($\approx +/-37°$). An angular correlation matrix has been created with the 90° detectors on one axis and the 37° detectors on the other axis. Gates have been set along both axes on the known $E2$ transitions. Energies, relative intensities, and angular correlation results (DCO) of the γ rays associated with the decay of ^{138}Nd are listed in Table I.

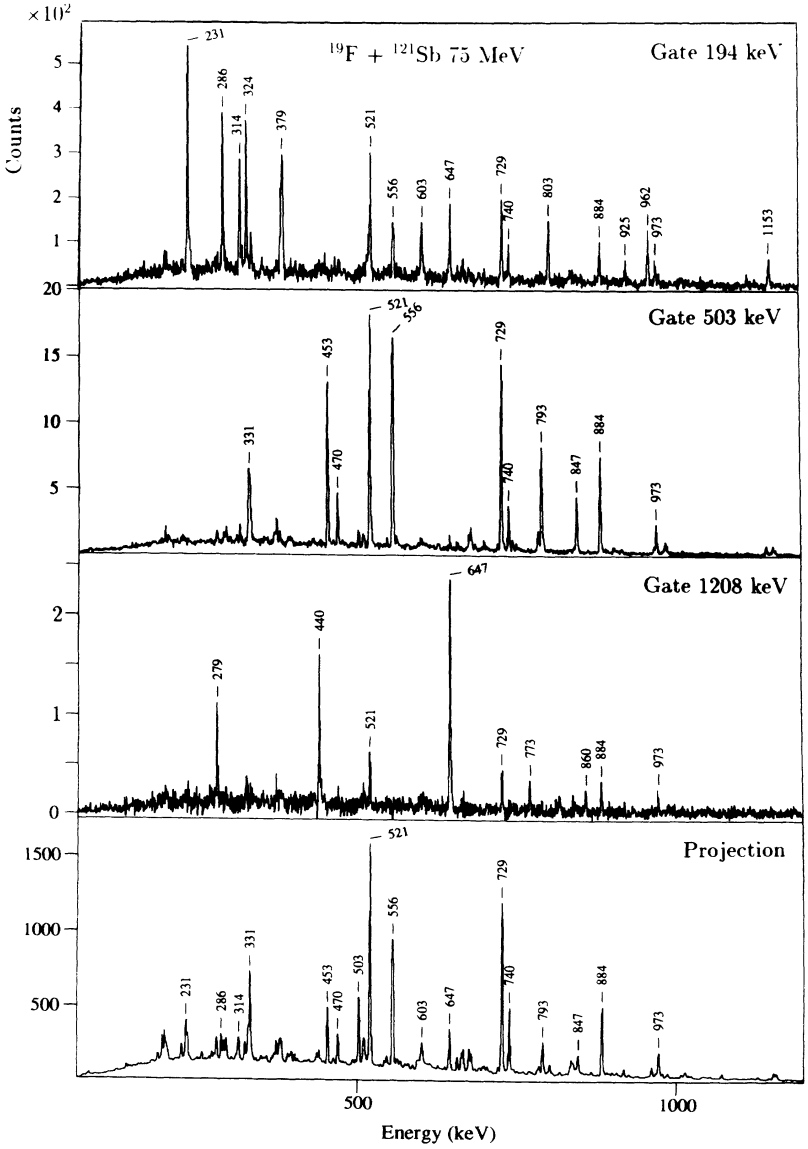

FIG. 1. Background corrected γ-γ coincidence spectra for selected transitions in ^{138}Nd.

III. THE LEVEL SCHEME OF ^{138}ND

The decay scheme of ^{138}Nd deduced from the present study is shown in Fig. 2. The data confirm the results reported in Ref. [6] up to the 3175 keV, 0.41 μs, 10^+ isomeric level. Above that state the level scheme is substantially modified and extended up to $\approx$ 8.5 MeV of excitation energy and $I = 21\hbar$. We have confirmed the 647.1–1208.0 keV coincidence relation above the 3175 keV state but we assign $I^\pi = 14^+$ to the level at 5030 keV on the basis of the angular correlation results when gating on the known 647 keV $E2$ transitions. At an excitation energy of 3.7 MeV a second 10^+ state has also been observed. It is populated by a cascade of four $E2$ transitions with energy spacings very similar to those of the ground-state band of the core nucleus ^{136}Ce. In contrast to Ref. [6], the 961.7 keV line appears to be parallel to the 647.1 keV transition and drains a new cascade of γ lines which, above 6 MeV, is characterized by a strong populated $\Delta I = 1$ band similarly as in the isotone ^{140}Sm [7].

IV. INTERPRETATION OF THE RESULTS

A. The ^{138}Nd nucleus and the $h_{11/2}$ proton and neutron alignment

The $N = 78$ nuclei of Sm, Gd, Dy [7,1,8] are characterized by two low-lying 10^+ excitations of mainly single

TABLE I. The ^{138}Nd γ-ray energies, relative γ intensities, and DCO ratios in the ^{121}Sb(^{19}F,4n) reaction at 75 MeV.

E_γ (keV)	Intensity[a]	DCO	E_x	Assignment	E_γ (keV)	Intensity[a]	DCO	E_x	Assignment
156.0(2)	7		5771	15→ 14	676.9(3)	92	0.40(5)	3372	$9^- \rightarrow 8^+$
187.0(2)	10	0.70(9)	2322	$7^- \rightarrow 6^+$	680.8(3)	84	0.90(10)	3247	$9^- \rightarrow 7^-$
193.8(2)	29	0.45(5)	5771	$15 \rightarrow 14$	701.2(3)	19	0.89(11)	2691	$7^- \rightarrow 5^-$
230.8(3)	40	0.38(5)	6002	$16^+ \rightarrow 15$	729.0(2)	1000	1.02(6)	1250	$4^+ \rightarrow 2^+$
231.0(3)	28	0.61(7)	2222	$5^- \rightarrow 5^-$	740.40(3)[b,c]			3915	$11^- \rightarrow 10^+$
278.0(4)	49	0.70(8)	5253	$13 \rightarrow 13$	740.6(3)[b,c]	353	0.60(7)	1190	$5^- \rightarrow 4^+$
278.6(4)	30	0.64(8)	5749	$16 \rightarrow 15$	747.5(3)	13	0.65(12)	5743	$15 \rightarrow 14^+$
286.3(2)	41	0.37(5)	2688	$(17) \rightarrow 16^+$	773.0(2)	26	0.92(12)	6243	$17 \rightarrow 15$
313.5(2)	46	0.68(7)	5253	$13 \rightarrow 12$	792.5(3)	163	1.08(11)	4996	$14^+ \rightarrow 12^+$
323.7(3)	35	0.51(6)	5577	$14 \rightarrow 13$	803.4(3)	66	0.70(8)	4940	$12 \rightarrow 11$
325.2(3)	22	0.69(8)	6568	$18 \rightarrow 17$	818.8(3)	9		6568	$(18) \rightarrow 16$
329.6(3)	54	0.68(7)	3700	$10^+ \rightarrow 9^-$	829.0(2)	8		1843	$4^+ \rightarrow 2^+$
331.4(3)	250	0.95(10)	2322	$7^- \rightarrow 5^-$	836.9(3)	69	0.93(10)	4752	$13^- \rightarrow 11^-$
369.3(3)	19	0.88(10)	2691	$7^- \rightarrow 7^-$	839.0(3)	18	0.93(12)	4211	$11^- \rightarrow 9^-$
372.8(3)	37	0.58(7)	2696	$8^+ \rightarrow 7^-$	847.4(3)	99	0.95(11)	5843	$16^+ \rightarrow 14^+$
379.1(3)[b]	30		7048	$(19) \rightarrow (18)$	860.4(3)	14		7428	$(19) \rightarrow (18)$
380.5(2)[b]	49	0.66(8)	6669	$(18) \rightarrow (17)$	884.4(2)	467	0.99(8)	2134	$6^+ \rightarrow 4^+$
390.9(2)	19	0.68(8)	3372	$9^- \rightarrow 8$	900.1(3)	6		5119	$\rightarrow 11^-$
438.0(2)	9		1454	$3^+ \rightarrow 2^+$	918.6(3)	51	0.99(10)	3240	$9^- \rightarrow 7^-$
440.1(2)	32	0.37(5)	5470	$15 \rightarrow 14^+$	924.7(3)	10	0.70(10)	8489	$(21) \rightarrow (20)$
453.6(2)	176	0.51(5)	3700	$10^+ \rightarrow 9^-$	961.7(3)	116	0.41(5)	4137	$11 \rightarrow 10^+$
469.6(2)	118	0.90(10)	1891	$7^- \rightarrow 5^-$	972.4(3)	98	90.52(6)	2222	$5^- \rightarrow 4^+$
493.1(2)	9		1014	$2^+ \rightarrow 2^+$	973.3(3)[b,c]			6002	$16^+ \rightarrow 14^+$
494.7(2)	16	1.09(13)	5470	$15 \rightarrow 13$	973.5(2)[b,c]	119	0.97	3108	$8^+ \rightarrow 6^+$
502.8(2)	227	0.99(10)	4203	$12^+ \rightarrow 10^+$	978.8(3)	22	0.96(13)	4219	$11^- \rightarrow 9^-$
516.7(2)	15	0.40(6)	7565	$(20) \rightarrow (19)$	986.9(3)	30	0.95(12)	6830	$18^+ \rightarrow 16^+$
520.8(2)	1000	1.00(7)	521	$2^+ \rightarrow 0^+$	1007.8(3)	28	1.06(14)	5760	$15 \rightarrow 13^-$
543.6(2)	20	0.88(10)	3915	$11^- \rightarrow 9^-$	1014.0(3)	10		1014	$2^+ \rightarrow 0^+$
555.8(3)[b]	345		3247	$9^- \rightarrow 8^+$	1019.4(3)	18	0.96(15)	5771	$15 \rightarrow 13^-$
556.9(3)[b]	368	0.77(9)	2691	$7^- \rightarrow 6^+$	1022.6(4)	10		5237	$\rightarrow 11^-$
562.2(2)	9	0.88(11)	2696	$8^+ \rightarrow 6^+$	1118.4(3)	10		4940	$12 \rightarrow 12^+$
602.6(2)	8		5577	$14 \rightarrow 13$	1146.6(3)	22	0.98(16)	5350	$14 \rightarrow 12^+$
627.9(3)	10	0.70(9)	6471	$(17) \rightarrow 16^+$	1153.2(4)	61	0.47(8)	4975	$13 \rightarrow 12^+$
639.5(3)	52	1.09(12)	5615	$14 \rightarrow 13$	1156.7(3)	23	1.02(20)	6152	$16 \rightarrow 14^+$
647.1(2)	108	1.09(11)	3822	$12^+ \rightarrow 10^+$	1208.0(3)	86	1.06(19)	5030	$14^+ \rightarrow 12^+$
659.1(2)	56	0.51(6)	2981	$8 \rightarrow 7^-$	1614.7(4)	35	0.64(15)	5437	$13 \rightarrow 12^+$
668.3(2)	80	0.99(10)	3915	$11^- \rightarrow 9^-$					

[a]Error on γ-ray intensities ranges between 10 and 40% depending on the intensity and complexity of the peaks.
[b]DCO value given for complex line.
[c]Transition intensity given for unresolved peak.

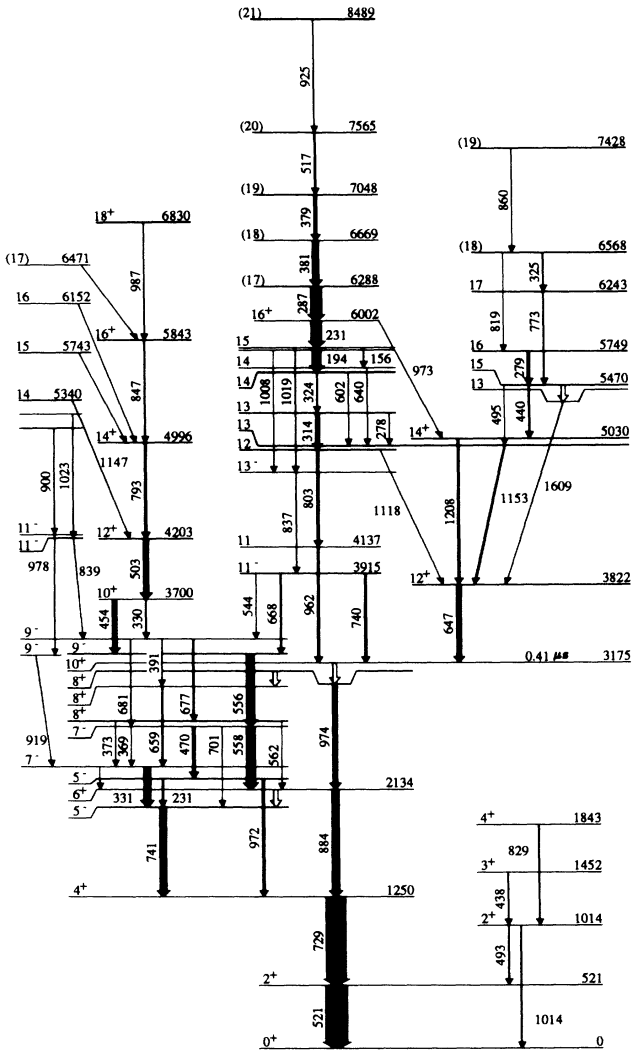

FIG. 2. Level scheme of ^{138}Nd deduced from the present work. The half-life of the 10^+ state at 3175 keV is taken from Ref. [6]. The assignments for the levels at 1014, 1452, and 1843 keV are taken from Ref. [28].

particle character at about the same excitation energy. These 10^+ states are also observed in the ^{138}Nd nucleus but, because of the lowering of the proton number and consequently of the lowering of the Fermi energy surface with respect to the $h_{11/2}$ proton orbital, we expect the $(\pi h^2_{11/2})_{10^+}$ to lie at higher energy compared to the 10^+ state of neutron character which should have constant energy in all the $N = 78$ isotones. We identify the 10^+ state at 3700 keV as the $\pi h^2_{11/2}$ configuration. The state indeed lies 0.5 MeV above the 3175 keV 10^+ level of neutron character. Once two neutrons are coupled to 10^+ we expect to see above it the energy spacings of the core nucleus whose excitations are due to the still available neutron hole pair.

In Fig. 3 we compare the $12^+ \rightarrow 10^+$ and the $14^+ \rightarrow 12^+$ energy spacings, 647.1 and 1208.0 keV, respectively, to the 2^+ and 4^+ excitation energies of the $^{140}Nd_{80}$ core [9]. We also show the comparison of the $E2$ γ cascade observed above the second 10^+ state at 3700 keV of excitation energy with the $N = 78$ ^{136}Ce core excitations [10]. Such good energy reproduction allows us to suggest for the second 10^+ state a proton configuration of particle-hole nature in which two proton particles are excited through the $Z = 64$ shell closure in the $h_{11/2}$ proton orbital. In fact, core excitations coupled to that state are then expected to be the $N = 78$ core vibrations due to the two still active pairs respect to the $N = 82$ shell closure. In Fig. 3 we also report the pertinent level sequences observed in the odd nuclei ^{137}Pr [11], $Z = 59$, and ^{139}Nd [12], $N = 79$, where a proton particle or a neutron hole are respectively excited in the $h_{11/2}$ orbital and coupled to the core states. All such cascades are examples of $\Delta I = 2$ decoupled bands built on single particle states whose behavior is representative of a shape transition from $N = 78$ to $N = 80$ nuclei [13].

B. Total Routhian surface calculations

To further elucidate the present data set, we performed cranked Strutinsky type calculations on a lattice in deformation space. These calculations are based on a Woods-Saxon potential [14] including a monopole pairing interaction. The energy in the rotating frame (Routhian) is minimized with respect to deformation parameters β_2, β_4, and γ. For more details we refer the reader to Refs. [15,16].

The total Routhian surface (TRS) of the ground state band (gsb) of ^{138}Nd is γ soft, showing only modest collectivity ($\beta_2 \approx 0.15$). With increasing frequency, the minimum corresponding to triaxial shape of $\gamma = -30°$ is becoming favored (Fig. 4). The first band crossing is calculated to be due to $h_{11/2}$ neutrons. The aligned $\nu(h_{11/2})^2$ configuration polarizes the core to a shape of $\gamma = -90°$, i.e., a shape similar to that of the gsb, where, however, most of the angular momentum is carried by the $h_{11/2}$ neutron pair along the noncollective axis of rotation.

At higher frequency, the $h_{11/2}$ protons align their angular momenta in a similar manner, driving the nucleus towards $\gamma = +30°$. The total Routhian surface calculations thus predict opposite driving force of protons and neutrons (see Fig. 4).

The sequence built on top of the $\pi(h_{11/2})^2$ configuration is of rotational character, showing a smooth gain in alignment. According to our calculations, this corresponds to the alignment of $h_{11/2}$ neutrons, where now the combined four quasiparticle configuration $\pi(h_{11/2})^2\nu(h_{11/2})^2$ favors prolate shape with rather small deformation $\beta_2 \approx 0.12$. The alignment gain is calculated respect to Harris parameters $J_0 = 14.0\hbar^2$ MeV^{-1} and $J_1 = 15.0\hbar^4$ MeV^{-3}. Since the band is observed only up to spin $18^+\hbar$, the full neutron alignment cannot be

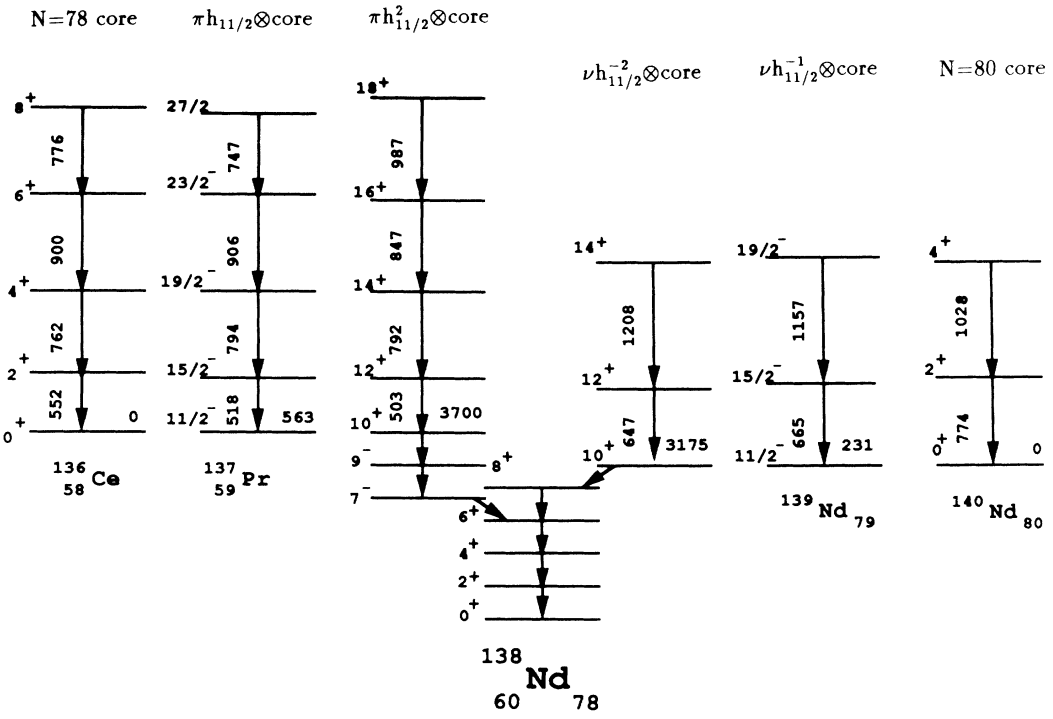

FIG. 3. Excited levels of the ^{138}Nd nucleus above the $h^2_{11/2}$ 10^+ states of proton and neutron character compared with the $N = 78$, 79, and 80 core excitations. The experimental data for ^{136}Ce, ^{137}Pr, ^{139}Nd, and ^{140}Nd nuclei are taken from Refs. [9–12].

extracted from the present data. More collective configurations are also expected, involving the $i_{13/2}$ excitation across the shell, but were not observed in the present experiment.

At higher angular momenta, a very interesting structure is observed, connected by $M1$ transitions only. The spin values are clearly suggestive of a four quasiparticle configuration and we suggest that this structure also involves the $\pi(h_{11/2})^2\nu(h_{11/2})^2$ quasiparticles. In contrast to the previous structure, where both neutrons and protons couple their angular momenta along the rotational axis, we suggest that only one kind of particle is coupled in that manner, whereas the other kind couples its angular momentum along the symmetry axis yielding a $K = 10^+$. The most probable configuration will correspond to $\pi(h_{11/2})^2\nu(h_{11/2})^2_{K=10^+}$ but the possibility of the protons to carry the high K cannot be excluded *a priori*. Indeed in the $A = 130$ mass region, similar rotational bands have been observed, connected via strong $M1$ transitions [17]. The structural assignment in general involves the rotational aligned neutrons, coupled to deformation aligned $h_{11/2}$ protons, which carry the high K [18]. In the isotone ^{136}Ce, a negative parity sequence of $M1$ transition has been interpreted in terms of $(\pi g_{7/2} - h_{11/2})_{K=9^-,8^-} - \nu(h_{11/2})^2$ [19]. The reason for us to prefer the case of the neutrons coupled to the high K relates to the fact that the structure built on top of the neutron 10^+ state shows no sign of collectivity. In contrast to the lighter isotopes, where the aligned neutrons favor collective oblate rotation, in heavier nuclei it seems that the $(h_{11/2})^2$ configuration is of little collectivity. On the other hand, the rotationally aligned protons, clearly induce collectivity at prolatelike shapes. From the $B(M1)/B(E2)$ ratios, one cannot easily distinguish between the two cases, since both are very large, although they are stronger in the case of high-K protons. Also the decay into the neutron 10^+ state speaks in favor of our assignment. However, only a g factor measurement would yield a definite answer.

A Fermi aligned coupling scheme for the $\pi(h_{11/2})^2\nu(h_{11/2})^2_{K=10^+}$ configuration yields a band-head spin of ≈ 14–$15\hbar$, in good agreement with what is seen in our data. The present structure resembles the recently observed $M1$ bands of the Pb region [20]. There the protons carry a large K value, whereas $i_{13/2}$ neutrons align their angular momentum along the rotational axis.

C. Interacting boson model plus broken pairs interpretation

The structure of high-spin states in ^{138}Nd can also be described in the framework of the interacting boson model (IBM) with broken pairs. The IBM [21] has been used mostly to describe low-spin states ($I \leq 10\hbar$) in nuclei. To extend its applicability to high-spin physics, one has to include part of the original shell-model fermion space through the breaking of the correlated S and D pairs. The model we have used for ^{138}Nd is described in detail in Refs. [22,23] and has been applied to transitional nuclei in the neutron deficient Sr-Zr-Mo region by Lister, Chowdhury, and Vretenar [24]. It is based on the IBM-1; the boson space consists of s and d bosons, with

no distinction between protons and neutrons. The model allows one or two bosons to be destroyed and form noncollective fermion pairs. High-spin states are described in terms of broken pairs. The model space for an even-even nucleus with $2N$ valence nucleons is

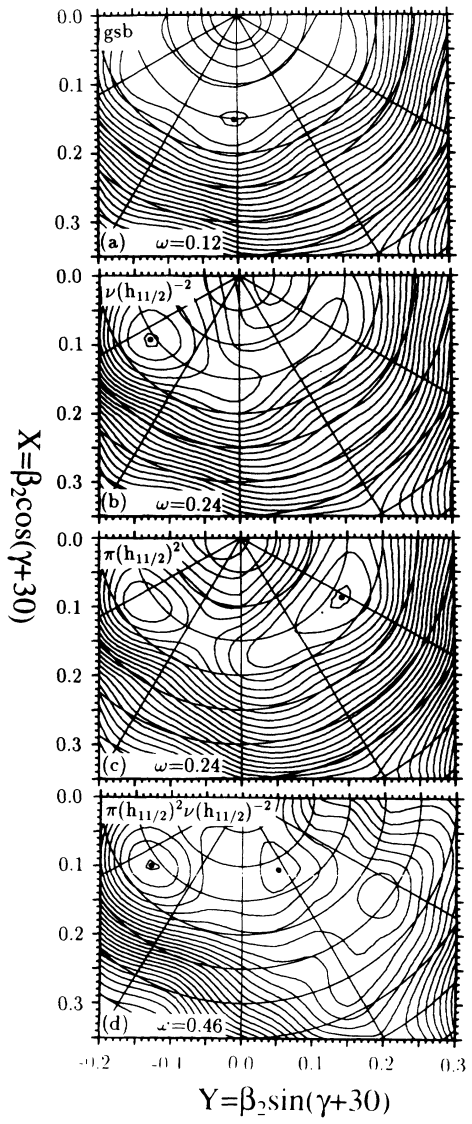

FIG. 4. Calculated total Routhian surfaces for relevant configurations of ^{138}Nd. (a) The vacuum configuration (ground-state band) revealing a very soft surface and a slight minimum at triaxial shape. (b) With increasing frequency, the neutrons align their angular momenta and drive the minimum towards triaxial shape ($\gamma = -90°$). (c) The excited surface of the $\pi(h_{11/2})^2$ configuration, showing opposite driving force than the neutrons ($\gamma = +30°$). The minimum at $\gamma = -90°$ corresponds to the $\nu(h_{11/2})^2$ configuration as in (b). (d) At high frequency a prolate minimum, corresponding to the four quasiparticle $\pi(h_{11/2})^2\ \nu(h_{11/2})^2$ coexists with the triaxial $\nu(h_{11/2})^2$ minimum. Note, however, that the spin at $\gamma = -90°$ is $\approx 13\hbar$ to be compared with $\approx 22\hbar$ at prolate shape. At the third minimum at large β_2 the $i_{13/2}$ neutrons become occupied.

$$|N \text{ bosons}\rangle \oplus |(N-1)\text{bosons} \otimes 1 \text{ broken pair}\rangle \oplus |(N-2)\text{bosons} \otimes 2 \text{ broken pairs}\rangle \ .$$

The one and two broken pairs are represented by two- and four-quasiparticle states that are coupled to the boson core. The model Hamiltonian has four terms: the IBM-1 boson Hamiltonian, the fermion Hamiltonian, the boson-fermion interaction, and a pair breaking interaction that mixes states with different number of fermions.

For ^{138}Nd we have used the set of parameters of the boson Hamiltonian: $\epsilon = 0.37$, $C_0 = 0.2$, $C_2 = -0.036$, $C_4 = 0.187$, $V_2 = 0$, and $V_0 = -0.2$ (all values in MeV). The number of bosons is $N = 7$. The boson parameters are very close to the values that are derived from an IBM-2 calculation for ^{136}Ce [25]. The resulting spectrum is close to the O(6) dynamical symmetry limit. The structure of high-spin states in ^{138}Nd is characterized by two $\Delta I = 2$ bands based on the two low-lying 10^+ states. According to the systematics of experimental data from neighboring nuclei, we expect the yrast two-quasiparticle (2qp) band to be a two-neutron band $(\nu h_{11/2})^2$, and the band based on the 10^+ state at 3700 keV to have a two-proton configuration $(\pi h_{11/2})^2$. Our model space does not include simultaneously protons and neutrons in broken pairs. Instead we have to perform two separate calculations: one for the neutron bands, and one with protons in the broken pairs. In both calculations we use the same boson core. In principle the fermions in broken pairs occupy the same set of valence orbitals from which the bosons are constructed. However, for the description of positive-parity bands close to the yrast line, the most important orbitals occupied by noncollective fermion pairs are the unique parity high-j orbitals. In order to reduce the large size of the fermion space, only the $h_{11/2}$ proton and neutron orbitals are included in the calculation of positive-parity bands. The single-quasiparticle energies and occupation probabilities are obtained by a simple BCS calculation using Kisslinger-Sorensen [26] single-particle energies and pairing strength $G = 23/A$. For the proton $h_{11/2}$ orbital: $v^2 = 0.03$ and $E = 1.75$ MeV. The occupation probability of the neutron $h_{11/2}$ orbital is $v^2 = 0.82$ and the BCS quasiparticle enegy is ≈ 1.1 MeV. This value is too low. To reproduce the excitation energy of the 10^+_1 state, we have to renormalize the value of $E_{\nu h_{11/2}}$ to 1.6 MeV.

The parameters of the boson-fermion interactions are determined from interacting boson-fermion model IBFM [27] calculations of low-lying negative-parity states in neighboring odd-A nuclei. For the proton states we consider $^{137}_{59}\mathrm{Pr}_{78}$ and $^{139}_{61}\mathrm{Pm}_{78}$. The corresponding odd-neutron nucleus is $^{139}_{60}\mathrm{Nd}_{79}$. In Fig. 5 we compare the negative-parity levels of these nuclei with results of model calculation. The decoupled structures are based on the $h_{11/2}$ proton and neutron orbitals. For ^{137}Pr we take as core nucleus ^{138}Nd, the occupation probability of the proton $h_{11/2}$ orbital is $v^2 = 0.05$ and the parameters of the boson-fermion interactions are $\Gamma_0 = 0.05$ MeV and $\chi = +1$ for the dynamical interaction, and $\Lambda_0 = 2.0$ MeV for the exchange interaction. For ^{139}Pm the core nucleus is ^{140}Sm, and the occupation probability and parameters

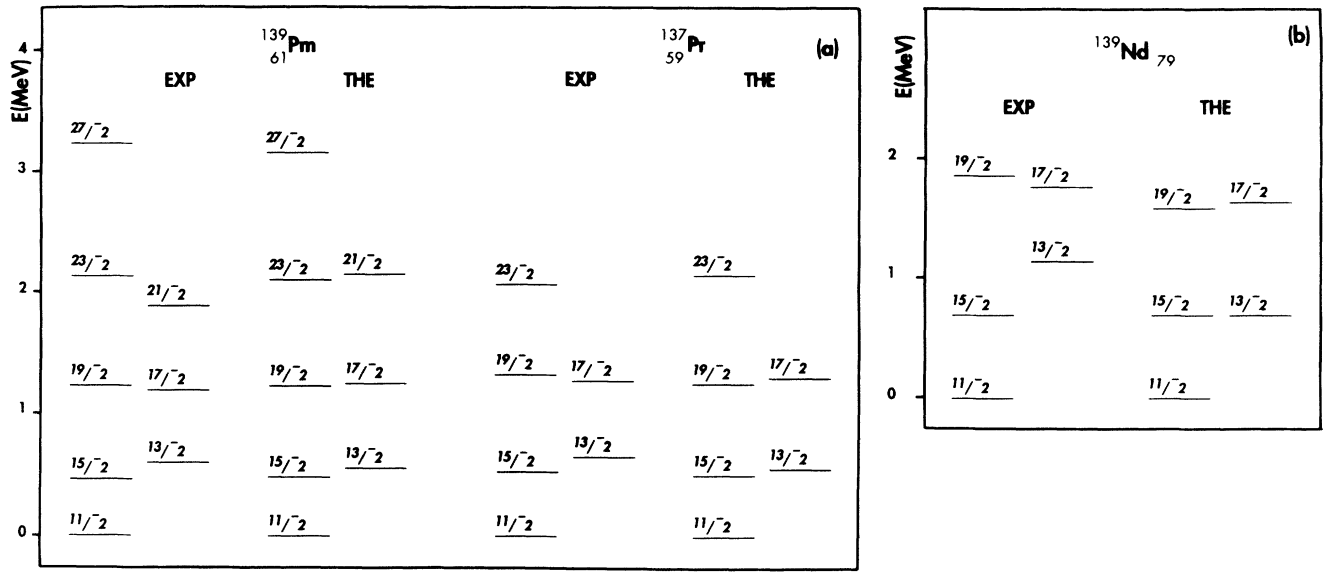

FIG. 5. Low-lying negative-parity states in (a) ^{139}Pm and ^{137}Pr and (b) ^{139}Nd compared with results of IBFM calcualtions. Excitation energies are relative to $E(11/2_1^-)$.

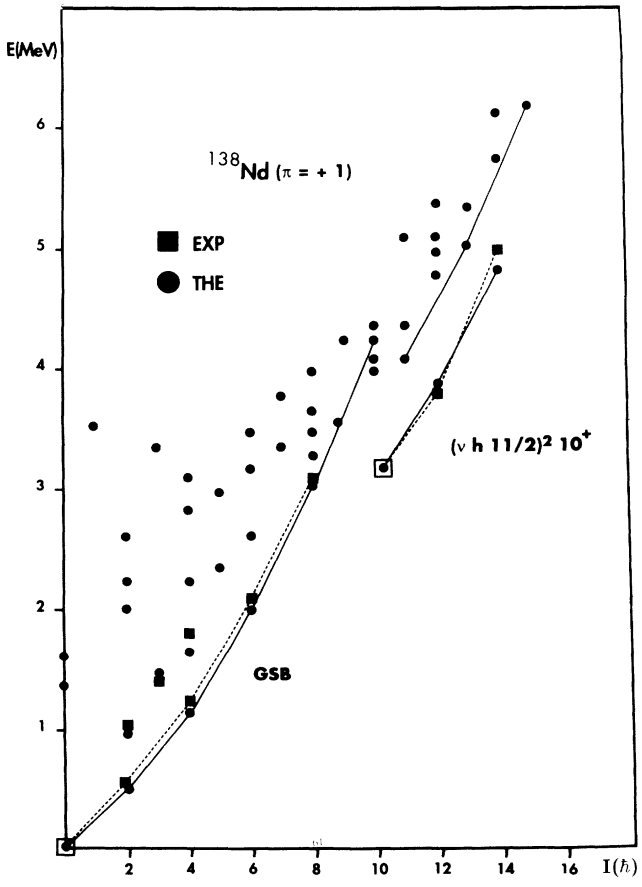

FIG. 6. Energy vs angular momentum diagram for calculated (circles) IBFM plus broken pair, and experimental (squares) yrast positive-parity states in ^{138}Nd.

of the boson-fermion interaction are the same as in ^{137}Pr. The core for ^{139}Nd is taken to be ^{138}Nd, $v^2(\nu h_{11/2}) = 0.82, \Gamma_0 = 0.4$ MeV, $\chi = -1, \Lambda_0 = 3.0$ MeV. The calculation reproduces well the experimental spectra for the two odd-proton nuclei [Fig. 5(a)] while for ^{139}Nd [Fig. 5(b)], we obtain the inversion $E(13/2_1^-) > E(15/2_1^-)$, but the large splitting between these levels is not reproduced by the calculation. This is probably due to our choice of the core nucleus: ^{138}Nd. From the discussion in the previous section it is clear that the correct core should be ^{140}Nd. However, our task is to describe the 2qp neutron bands in ^{138}Nd, where the core is obviously ^{138}Nd (with one boson less). In this sense the present IBFM calculation gives the best boson-fermion parameters to be used in ^{138}Nd. The strength parameter of the pair-breaking interaction in ^{138}Nd is $U_2 = 0.2$ MeV for both proton and neutron states.

In Fig. 6 we display the results of model calculation for ^{138}Nd with neutrons in broken pairs. For simplicity, the model space contains only one broken pair $(h_{11/2})^2$. Only few lowest levels of each spin are shown in the energy vs angular momentum diagram. The calculated levels are compared with the experimental yrast states. The collective ground-state band is the yrast band up to angular momentum $I = 8^+$. The calculation reproduces the experimental positions of states of the ground-state band, as well as the excitation energies of the states 2_2^+, 3_1^+, and 4_2^+. The two neutron band $(h_{11/2})^2$ becomes the yrast band at the state 10_1^+. Only the first three states of this band are seen experimentally. The calculated levels reproduce the correct excitation energies. The main components in the wave functions of the states of this band are $|(\nu h_{11/2})^2 J_F = 10, I_B; I = J_F + I_B\rangle$, where $|I_B\rangle$ denotes a collective state of the boson system be-

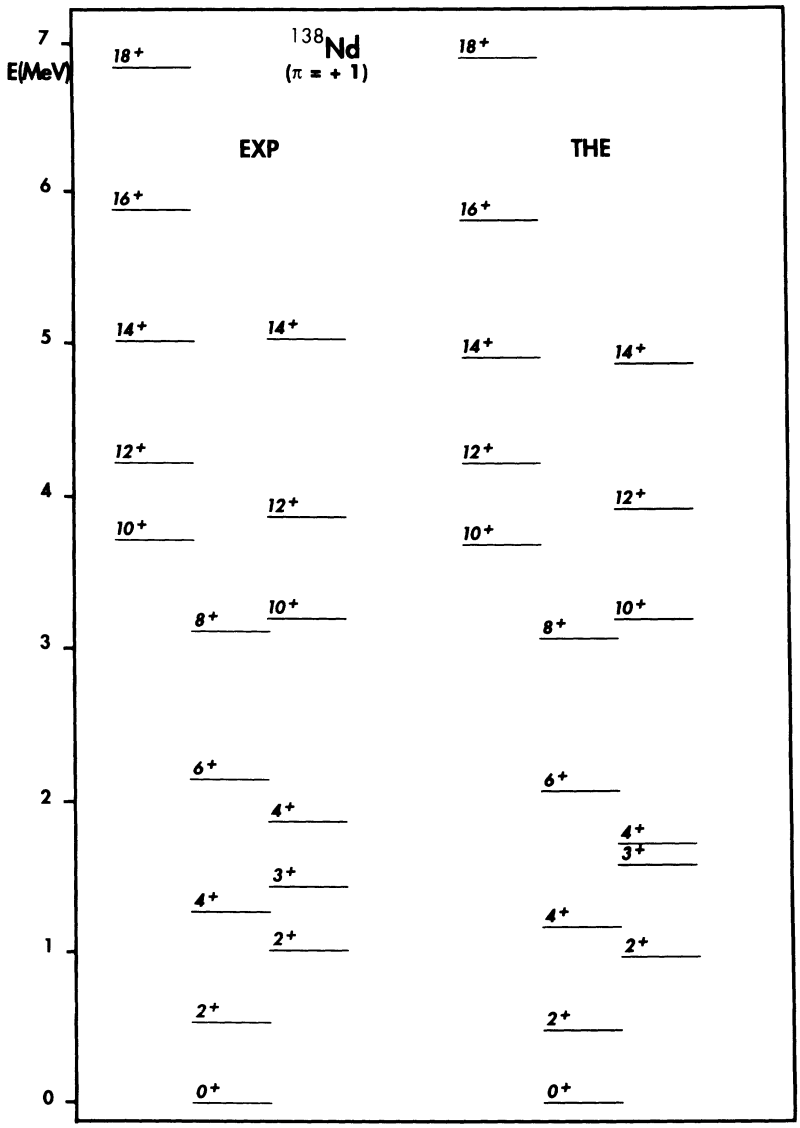

FIG. 7. Comparison between experimental and calculated positive-parity levels in ^{138}Nd.

longing to the ground-state band with angular momentum I_B. The two $h_{11/2}$ neutrons are completely decoupled from the core and align their angular momenta along the axis of rotation. The fermion angular momentum J_F is a good quantum number for 2qp states close to the yrast line. Above the yrast we follow the odd-spin band $|(\nu h_{11/2})^2 J_F = 10, I_B; I = J_F + I_B - 1\rangle$. This band is not seen in the experiment. For states higher above the yrast line the Coriolis mixing is much stronger and classification into bands is no longer possible. In Fig. 7 we compare in a more usual form the lowest calculated levels with experimental data. Here the two-proton band $|(\pi h_{11/2})^2 J_F = 10, I_B; I = J_F + I_B\rangle$ is also displayed. The proton states are obtained in a separate calculation, that is, there is no mixing between two-proton and two-neutron states. It is seen that the calculated two-proton band reproduces the corresponding experimental levels up to the highest observed member of this band: 18^+. The agreement between calculated and experimental levels is better than for the two-neutron band $(h_{11/2})^2_{10^+}$. The reason is that the transition energies in the two-proton band are very similar to the energy spacings in the ground-state band. The transition energies in the two-neutron band follow the ground-state band in ^{140}Nd, rather than in ^{138}Nd.

The structure of negative-parity states in ^{138}Nd is more complex. We have calculated the negative-parity two neutron states and compared them with experimental levels in Fig. 8. In addition to $h_{11/2}$, the $d_{3/2}$ neutron orbital is included in the model space. $v^2_{d3/2} = 0.2$ and $E_{d3/2} = 0.95$ MeV. The parameters of the Hamiltonian have the same values as in the calculation of positive-parity two-neutron bands, except for Γ_0, the strength of the dynamical boson-fermion interaction, which has been slightly increased from 0.4 to 0.5 MeV. Due to the fact that $v^2_{d3/2} < 0.5$ and $v^2_{h11/2} > 0.5$, the lowest negative-parity structure is the parabola (open up) of

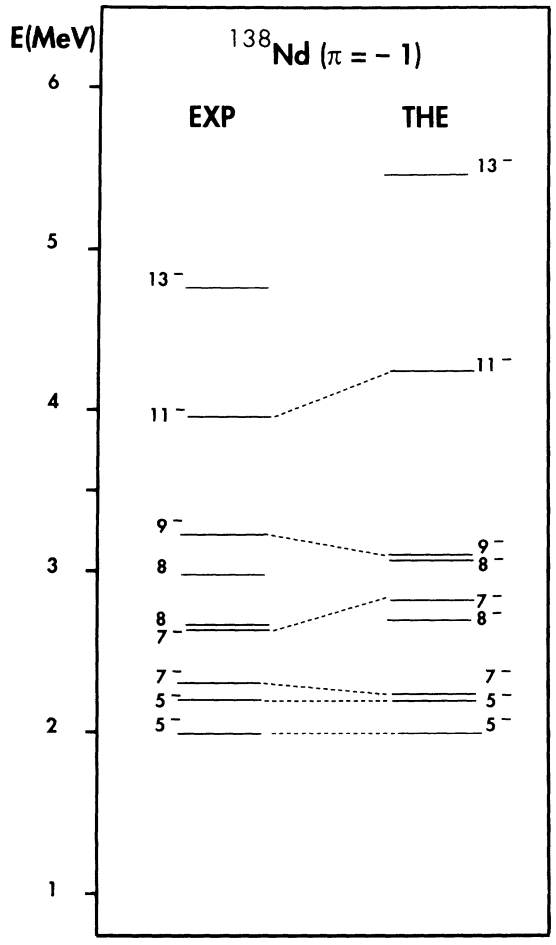

FIG. 8. Experimental negative-parity states in ^{138}Nd compared with results of model calculation (IBFM plus broken pair).

states $(h_{11/2}, d_{3/2})J_F = 4, 5, 6, 7$ coupled to the ground state $|I_B = 0\rangle$ of the core. The lowest member of the parabola is the state 6^- (not shown in the figure) at 1.86 MeV. In Fig. 8 we display only those calculated states that have a possible experimental counterpart. The density of negative-parity states in the region $E \approx 2$–4 MeV is high. The states 5_1^- and 7_1^- belong to the lowest parabola. The level 5_2^- is predominantly a one d boson state with the main components in the wave function: $|(h_{11/2}, d_{3/2})4, I_B = 2, 5^-\rangle$ and $|(h_{11/2}, d_{3/2})6, I_B = 2; 5^-\rangle$. Above the lowest parabola angular momentum is generated by coupling $(h_{11/2}, d_{3/2})$ to the ground-state band of the core (states $8_1^-, 9_1^-, 11_1^-, 13_1^-$).

Another distinct high-spin structure in ^{138}Nd is the sequence of $\Delta I = 1$ transitions extending up to $I^\pi = (21)$ at 8.5 MeV. We have not been able to reproduce this band in our calculations. By extending the model space to include one- and two-broken pairs (2qp and 4qp), we have investigated the possibility that these states belong to a four-neutron or four-proton band. In all our calculations the lowest 4qp states are grouped into $\Delta I = 2$ bands, with signature partners (states that have the same collective structure, but opposite signature) lying very close to each other. The observed band, as already noticed, will probably represent four quasiparticle proton-neutron excitations that are not included in our model space.

V. CONCLUSIONS

In conclusion, we have studied the high spin structure of the transitional nucleus ^{138}Nd up to $I = 21\hbar$ and to 8.5 MeV of excitation energy. The rich level structure which is observed above the 10^+ states can be well understood if one considers the coupling of two protons or two neutrons in the $h_{11/2}$ state to different core excitations. Such configurations give rise to collective bands that are representative of different core deformations due to the polarizing effects of the valence particles.

The behavior of the core collectivity is analyzed in the framework of the cranked Strutinsky calculations on a lattice (TRS) and has a natural explanation in an extended IBFM model which incorporates broken boson pairs.

[1] W. Starzecki, G. de Angelis, B. Rubio, J. Styczen, K. Zuber, H. Güven, W. Urban, W. Gast, P. Kleinheinz, S. Lunardi, F. Soramel, A. Facco, C. Signorini, M. Morando, W. Meczynsky, A. M. Stefanini, and G. Fortuna, Phys. Lett. B **200**, 419 (1988).

[2] D. Bazzacco, F. Brandolini, K. Löwenich, S. Lunardi, P. Pavan, C. Rossi-Alvarez, F. Soramel, M. De Poli, A. M. I. Haque, and G. de Angelis, Phys. Lett. B **206**, 404 (1988).

[3] R. Wyss, A. Granderath, R. Bengtsson, P. von Brentano, A. Dewald, A. Gelber, A. Gizon, J. Gizon, S. Harrissopulos, A. Johnson, W. Lieberz, W. Nazarewicz, J. Nyberg, and K. Schiffer, Nucl. Phys. **A505**, 337 (1989).

[4] Y. S. Chen, S. Frauendorf, and G. A. Leander, Phys. Rev. C **28**, 2437 (1983).

[5] E. S. Paul, D. B. Fossan, Y. Liang, R. Ma, N. Xu, R. Wadsworth, I. Jenkins, and P. J. Nolan, Phys. Rev. C **41**, 1576 (1990).

[6] M. Müller-Veggian, H. Beuscher, D. R. Haenni, R. M. Lieder, A. Neskakis, and C. Mayer-Böricke, Nucl. Phys. **A344**, 89 (1980).

[7] S. Lunardi, D. Bazzacco, G. Nardelli, F. Soramel, J. Rico, E. Maglione, M. De Poli, and G. de Angelis, Phys. Rev. C **42**, 174 (1990).

[8] D. Bazzacco, S. Lunardi, F. Soramel, M. A. Cardona, M. De Poli, G. de Angelis, F. Terrasi, V. Roca, A P. H. Gracie, and P. Simmons, LNL-INFN Report No. 047/91.

[9] L. K. Peker, Nucl. Data Sheets **51**, 425 (1987).
[10] T. W. Burrows, Nucl. Data Sheets **52**, 273 (1987).
[11] L. K. Peker, Nucl. Data Sheets **59**, 767 (1990).
[12] T. W. Burrows, Nucl. Data Sheets **57**, 337 (1989).
[13] P. Kleinheinz (private communication).
[14] S. Ćwiok, J. Dudek, W. Nazarewicz, J. Skalski, and T. Werner, Comput. Phys. Commun. **46**, 379 (1987).
[15] W. Nazarewicz, R. Wyss, and A. Johnsson, Nucl. Phys. **A503**, 285 (1989).
[16] R. Wyss, J. Nyberg, A. Johnson, R. Bengtsson, and W. Nazarewicz, Phys. Lett. B **215**, 211 (1988).
[17] E. S. Paul, C. W. Beausang, D. B. Fossan, R. Ma, W. F. Piel, Jr., N. Xu, L. Hildingsson, and G. A. Leander, Phys. Rev. Lett. **58**, 984 (1987).
[18] D. B. Fossan, J. R. Hughes, Y. Liang, R. Ma, E. S. Paul, and N. Xu, Nucl. Phys. **A520**, 241 (1990).
[19] E. S. Paul, D. B. Fossan, Y. Liang, R. Max, N. Xu, R. Wadsworth, I. Jenkins, and P. J. Nolan, Phys. Rev. C **41**, 1576 (1990).
[20] R. M. Clark, R. Wadsworth, E. S. Paul, C. W. Beausang, I. Ali, A. Astier, D. M. Cullen, P. J. Dagnall, P. Fallon, M. J. Joyce, M. Meyer, N. Redon, P. H. Regan, W. Nazarewicz, and R. Wyss, Phys. Lett. B **275**, 247 (1992).
[21] F. Iachello and A. Arima, *The Interacting Boson Model* (Cambridge Univ. Press, Cambridge, 1987).
[22] F. Iachello and D. Vretenar, Phys. Rev. C **43**, 945 (1991).
[23] D. Vretenar, G. Bonsignori, and M. Savoia, Phys. Rev. C **47**, 2019 (1993).
[24] C. J. Lister, P. Chowdhury, and D. Vretenar, Nucl. Phys. **A557**, 361 (1993).
[25] O. Scholten, Ph.D. thesis, University of Groningen, 1980.
[26] L. S. Kisslinger and R. A. Sorensen, Rev. Mod. Phys. **35**, 853 (1963).
[27] F. Iachello and O. Scholten, Phys. Rev. Lett. **43**, 679 (1979); F. Iachello and P. Van Isacker, *The Interacting Boson-Fermion Model* (Cambridge Univ. Press, Cambridge, 1991).
[28] J. K. Tuli, Nucl. Data Sheets **69**, 69 (1993).